

Techno-economic environmental and social assessment framework for energy transition pathways in integrated energy communities: a case study in Alaska

Jayashree Yadav, *Member, IEEE*, Ingemar Mathiasson, Bindu Panikkar
and Mads Almassalkhi, *Senior Member, IEEE*

Abstract—The transition to low-carbon energy systems demands comprehensive evaluation tools that account for technical, economic, environmental, and social dimensions. While numerous studies address specific aspects of energy transition, few provide an integrated framework that captures the full spectrum of impacts. This study proposes a comprehensive techno-economic, environmental, and social (TEES) assessment framework to evaluate energy transition pathways. The framework provides a structured methodology for assessing infrastructure needs, cost implications, emissions reductions, and social equity impacts, offering a systematic approach for informed decision-making. To illustrate its applicability, a detailed case study of a remote community in Alaska is conducted, evaluating the TEES impacts of three distinct energy transition pathways including heat pumps (HPs) and battery integration, resource coordination and expanded community solar photovoltaic (PV). Findings show that coordination of HPs minimizes peak demand, enhances grid reliability, and reduces energy burdens among low-income households. Extensive simulation-based analysis reveals that strategically staging electric HPs with existing oil heating systems can lower overall energy costs by 19% and reduce emissions by 29% compared to the today’s system and outperforms all-heat-pump strategy for economic savings. By combining a generalizable, community-centric assessment framework with data-driven case study insights, this work offers a practical tool for utilities, community stakeholders and policymakers to work toward equitable and sustainable energy transitions.

Index Terms—Energy transition, Carbon emission, Heat pumps, Energy burden, Energy poverty, Techno-economic, Microgrids

I. INTRODUCTION

The global energy sector is undergoing a fundamental shift from fossil fuel-based systems toward decarbonized energy solutions in response to climate change, as outlined in the 2015 Paris Agreement. Renewable energy sources such as wind, solar, and biomass are increasingly replacing traditional fossil fuel and nuclear power generation [1]. Over the past decade,

research on green energy transitions has grown substantially, addressing the pace of transitions [2], [3], [4], alternative pathways [5], [6], [7], and the geographic dimensions of energy transitions [8], [9]. Transition scenarios vary significantly across regions, particularly in extreme climates where infrastructure, resource availability, and energy costs present unique challenges [9].

Remote northern integrated energy communities face distinct technical, economic, and social barriers to adopting renewable energy [10]. These communities often rely on isolated diesel-powered microgrids, resulting in high electricity costs, supply chain vulnerabilities, and carbon-intensive power generation [11]. Additionally, heating demand in such regions can be 1.5 to 2 times higher than electricity demand [12], further increasing dependence on imported fuels. The extreme climate—marked by extended summer daylight and prolonged winter darkness—adds complexity to renewable deployment, storage strategies, and grid reliability. These unique conditions require integrated assessment frameworks that consider not only technical and economic aspects, but also environmental sustainability and social equity.

To support effective decision-making, community-centric assessment frameworks that capture multi-sectoral interactions are essential [13]. Much of the existing literature focuses on techno-economic analysis of specific technologies, such as photovoltaic thermal systems [14], electric vehicle chargers [15], or rooftop PV [16]. While informative, these studies often overlook broader environmental and social considerations. For example, [17], [18] include environmental criteria but exclude social dimensions, whereas [19] focus on socio-economic indicators without addressing grid performance. Though some studies incorporate multiple dimensions, such as [20], which evaluates hybrid energy systems in Chad, they emphasize optimal sizing over real-time energy management and lack integration of end-use technologies like heat pumps or demand-side flexibility. Moreover, many analyses are simulation-based and not grounded in real-world data.

Among the strategies for decarbonization, electrification of end-use sectors such as transportation and space heating plays a vital role. Heat pumps, in particular, offer significant potential to reduce greenhouse gas emissions while improving energy efficiency [21]. Studies have shown their benefits in reducing emissions [22], [23], enhancing grid flexibility

Corresponding author: Jayashree Yadav.

Jayashree Yadav and Mads Almassalkhi are with the College of Engineering and Mathematical Science; Gund Institute for Environment, University of Vermont, Burlington 05401, USA (e-mail: jayadav@uvm.edu; malmassa@uvm.edu).

Ingemar Mathiasson is Department of Energy, Northwest Arctic Borough, Kotzebue 99752, Alaska, USA (e-mail: imathiasson@nwabor.org).

Bindu Panikkar is with Rubenstein School of the Environment and Natural Resources; Gund Institute for Environment, University of Vermont, Burlington 05401, USA. (e-mail: Bindu.Panikkar@uvm.edu).

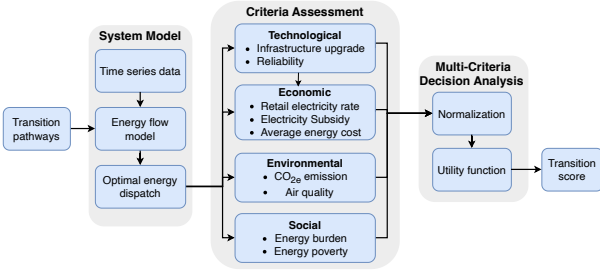


Fig. 1. Transition pathways assessment framework

[24], [25], and lowering operational costs [21], [26]. However, widespread adoption also presents challenges, including high upfront costs, grid integration issues, and energy equity concerns [27], [28]. Notably, many studies assume constant coefficients of performance (COP) for heat pumps, which can misrepresent their performance in cold climates [22], [23], [25]. Recent findings underscore the importance of temperature-dependent COPs to accurately assess heating system economics and performance [29].

The key contributions of this manuscript to address these research gaps are as follows:

- Develops a comprehensive techno-economic, environmental, and social (TEES) assessment framework to evaluate energy transition pathways that can integrate intelligent energy devices and optimization-based coordination of energy assets.
- Applies the framework to a detailed case study of a remote community in Alaska, evaluating the TEES impacts of three distinct energy transition pathways, including heat pump and battery integration, resource coordination, and expanded community solar PV, compared to the community’s baseline (today’s) system.
- Through extensive simulation-based analysis, we demonstrate how to strategically stage electric heat pumps with existing oil heating systems to reduce overall energy costs by 17-19% and emissions by 27-29% when compared with today’s system and outperforms the all-heat-pump strategy for economic savings.

The rest of the article is organized as follows: Section II outlines the transition pathway assessment framework in detail. Section III presents the application of the framework to a remote community in Alaska. Section IV provides results for different transition pathways, followed by a comparative discussion in Section V, focusing on the technological, economic, environmental, and social impacts of each transition pathway. Finally, the article concludes with a summary of key findings.

II. TRANSITION PATHWAYS ASSESSMENT FRAMEWORK

Fig. 1 presents the proposed TEES assessment framework. Each transition pathway is analyzed using a system model, which includes input data, an energy flow model and optimal energy dispatch to generate system-wide energy response. This information is then analyzed within the criteria assessment module, which evaluates TEES impacts. Finally, a multi-criteria decision analysis (MCDA) approach is applied to

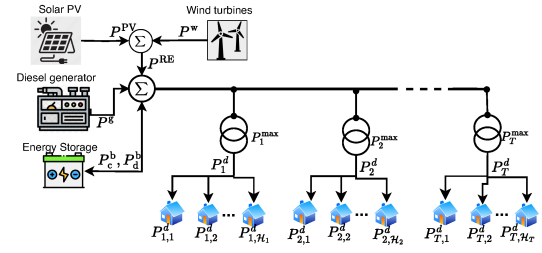


Fig. 2. Electrical system block diagram of an integrated energy community
normalize the assessed criteria and compute a transition score for each pathway.

A. System Model

A typical electricity distribution system for an energy community is illustrated in Fig. 2. The system comprises a diesel generator as the primary power source, supplemented by renewable energy sources – solar PV, wind power, and an energy storage system. Electricity generated from these sources is distributed to consumers through transformers, each serving a specific group of residential or commercial loads.

1) *Energy flow model*: The electricity distribution system can be modeled as an energy flow model. The model assumes a lossless distribution system, with power balance equations governing the energy flow, as expressed in (1). Equation (1a) represents the power balance at each time step k , where the total demand is met by power generation from diesel (P^G), renewable energy ($P^{RE} = P^{PV} + P^W$), and battery discharge (P_d^b), while battery charging (P_c^b) is treated as a load. Equation (1b) defines the demand at transformer τ as the sum of individual household loads $P_{\tau,h}^d$ connected to it. The sets K , T , and \mathcal{H}_τ represent discrete time instants, transformers in the system, and houses connected to transformer τ , respectively. The power flow components— $P^G \in [0, P_{\max}^G]$, P^{RE} , $P_d^b \in [0, P_{\max}^b]$, P_c^b , and $P^d \in [0, P_{\max}^d]$ —are determined through individual component models, optimal dispatch algorithms, and coordination strategies.

$$\sum_{\tau=1}^T P_{\tau}^d[k] = P^G[k] + P^{RE}[k] + P_d^b[k] - P_c^b[k] \quad \forall k \in K \quad (1a)$$

$$P_{\tau}^d[k] = \sum_{h=1}^{\mathcal{H}_{\tau}} P_{\tau,h}^d[k] \quad \forall \tau \in T, \quad \forall k \in K \quad (1b)$$

a) *Diesel Generator (P^G)*: The diesel generator is modeled using a cost curve, which defines the relationship between fuel consumption cost and power generation. This curve is derived from the generator heat rate curve, obtained from the NREL data catalog for diesel generators [30]. The generator cost curve is then computed from the heat rate curve using the methodology outlined in Chapter 11 of [31].

b) *Renewable Energy Injection (P^{RE})*: Renewable energy generation can be incorporated either as available data or through models based on irradiance or wind flow when data is unavailable. In this work, power generation data for existing renewable energy resources was available and directly utilized.

For scenarios with increased renewable capacity, the generated power is scaled as follows:

$$P_{\text{new}}^{\text{RE}}[k] = P_{\text{base}}^{\text{RE}}[k] \cdot M \quad \forall k \in K, \quad (2)$$

where $P_{\text{new}}^{\text{RE}}$ and $P_{\text{base}}^{\text{RE}}$ represent the scaled and original power generated from renewable sources, respectively, and M is the capacity scaling factor.

c) *Battery Model (P^b)*: For battery, this work employs the Energy Reservoir Model (ERM), which is commonly used in system-level research. The battery's State of Charge (SoC), denoted by $E[k] \in [\underline{E}, \overline{E}]$, evolves according to the charging (P_c^b) and discharging (P_d^b) powers. The ERM model is mathematically represented as follows:

$$E[k+1] = E[k] + \frac{\Delta t}{E_C} (\eta^b P_c^b[k] - \frac{1}{\eta^b} P_d^b[k]) \quad \forall k \in K, \quad (3a)$$

$$P_c^b[k] = P_{\text{max}}^b z[k]; P_d^b[k] = P_{\text{max}}^b (1 - z[k]) \quad \forall k \in K, \quad (3b)$$

where E_C is the energy capacity of the battery in kWh and η^b is battery efficiency, K is sample size and Δt is time step between two samples. Additionally, the complementarity constraints in (3b) ensure that the battery cannot be charged and discharged simultaneously.

d) *Household demand model (P^d)*: The household demand in (4) is modeled as the sum of the base demand (D) and the additional power consumption (P^{HP}) associated with the controllable loads.

$$P_{\tau,h}^d[k] = D_{\tau,h}[k] + P_{\tau,h}^{\text{HP}}[k] \quad \forall k \in K, \forall h \in \mathcal{H}_\tau, \tau \in \mathbf{T}, \quad (4)$$

where K , \mathbf{T} , and \mathcal{H}_τ denote the sets of time steps, transformers, and households connected to transformer τ . D is provided as data, while P^{HP} is obtained through modeling. Though HPs are the focus here, the same formulation applies to ACs by replacing Q^a with $-Q^a$, or to other loads using appropriate models.

HPs are modeled using the Equivalent Thermal Parameter (ETP) model, which computes indoor temperature using household parameters and HP energy flow [32].

$$T^a[k+1] = \frac{\Delta t}{C^a} (T^m[k] H^m - (U^a + H^m) T^a[k] + T^o[k] U^a + Q^a), \quad (5a)$$

$$= \frac{\Delta t}{C^a} (T^m[k] H^m - (U^a + H^m) T^a[k] + T^o[k] U^a + P^{\text{HP}}[k] \cdot \text{COP}[k] + Q^{\text{oil}}[k]),$$

$$T^m[k+1] = \frac{\Delta t}{C^m} (H^m (T^a[k] - T^m[k]) + Q^m). \quad (5b)$$

Here, T^a and T^m are indoor air and mass temperatures, C^a and C^m are thermal capacities, U^a is the envelope conductance, H^m is the conductance between air and mass, and T^o is outdoor temperature. Q^m , heat flux to the interior mass, is set to zero for simplicity.

The heat delivered, Q^a , includes HP output and oil-based heating: $Q^a = \text{COP} \cdot P^{\text{HP}} + Q^{\text{oil}}$. COP, which measures HP efficiency, varies with outdoor temperature and drops significantly in cold climates [33]. When T^o drops below the cutoff T_{min}^o , oil heating (Q^{oil}) is used instead. This study models inverter-driven HPs, treating P^{HP} as a continuous variable.

2) *Optimal energy dispatch*: The optimal dispatch algorithm computes generator (P^g) and battery (P^b) schedules to minimize generation cost ($\alpha P^g[k]$), subject to power balance, SOC limits, and battery operating constraints (6). Inputs include renewable generation (P^{RE}) and demand (P^d), while P^g and P^b are decision variables. The cost coefficient α is based on the generator's cost curve, and γ penalizes large generator fluctuations. Constraint (6j) ensure full battery cycles under warm conditions for effective utilization.

Demand P^d depends on the transition pathway, appliance size, and coordination method. It is given by (7d), where D is the base demand and P^{HP} is the additional controlled load. The optimization problem is formulated as:

$$\min_{P^g, P_c^b, P_d^b} \alpha \sum_{k=1}^K P^g[k] + \gamma \sum_{k=1}^{K-1} (P^g[k+1] - P^g[k])^2, \quad (6a)$$

subject to:

$$P^d[k] + P_b^c[k] = P^g[k] + P^{\text{RE}}[k] + P^w[k] + P_d^b[k] \quad \forall k \in K, \quad (6b)$$

$$E[k+1] = E[k] + \frac{\Delta T}{E_C} (\eta^b P_c^b[k] - \frac{1}{\eta^b} P_d^b[k]) \quad \forall k \in K, \quad (6c)$$

$$P_c^b[k] \leq P^{\text{PV}}[k] + P^g[k] \quad \forall k \in K, \quad (6d)$$

$$0 \leq P^g[k] \leq P_{\text{max}}^g[k] \quad \forall k \in K, \quad (6e)$$

$$P_c^b[k] = P_{\text{max}}^b z[k]; P_d^b[k] = P_{\text{max}}^b (1 - z[k]) \quad \forall k \in K, \quad (6f)$$

$$0 \leq P_c^b[k], P_d^b[k] \leq P_{\text{max}}^b, \quad z = \{0, 1\} \quad \forall k \in K, \quad (6g)$$

$$\underline{E} \leq E[k+1] \leq \overline{E} \quad \forall k \in K, \quad (6h)$$

$$E[1] = E[K+1], \quad (6i)$$

$$T_s \sum_{k \in N_{\text{day}}} P_c^b[k] \eta^b \geq E_C, \quad T_s \sum_{k \in N_{\text{day}}} P_d^b[k] / \eta^b \geq E_C$$

include if $\min_{k \in N_{\text{day}}} \{T^o[k]\} > T_{\text{warm}}^o, \quad (6j)$

3) *Intelligent coordination*: In the optimal dispatch, demand can be predefined (base) or dynamically determined via intelligent coordination of energy-efficient appliances. This section formulates heat pump coordination to minimize transformer loading.

The objective (7a) minimizes transformer load P_τ at each time step k , while (7b) limits transformer load to its rated power. Constraint (7c) ensures total demand (P^d)—sum of base demand (D) and HP power (P^{HP})—does not exceed available generation. Equations (7e)–(7f), and (7k) model the ETP-based thermal dynamics with heating from heat pumps or oil. Stove oil is used, and Q_{oil} is computed using EIA-specified energy density. Indoor temperature continuity across days is maintained by initializing with the previous day's final value.

$$\min_{P^{\text{HP}}} \sum_{\tau \in \mathbf{T}} P_\tau[k] \quad (7a)$$

subject to:

$$D_\tau[k] + \sum_{h \in \mathcal{H}_\tau} P_{\tau,h}^{\text{HP}}[k] \leq P_\tau[k], \quad \forall k \in K, \forall \tau \in \mathbf{T} \quad (7b)$$

$$P^d[k] \leq P_{\text{max}}^g + P^{\text{PV}}[k] \quad \forall k \in K \quad (7c)$$

$$P^d[k] = \sum_{\tau \in \mathbf{T}} \left(D_\tau[k] + \sum_{h \in \mathcal{H}_\tau} P_{\tau,h}^{\text{HP}}[k] \right) \quad (7d)$$

$$T_{\tau,h}^a[k+1] = T_{\tau,h}^a[k] + \frac{\Delta t}{C_{\tau,h}^a} \left(T_{\tau,h}^m[k] \cdot H_{\tau,h}^m - T_{\tau,h}^a[k] \cdot (U_{\tau,h}^a + H_{\tau,h}^m) + T_{o,k} \cdot U_{\tau,h}^a + P_{\tau,h}^{\text{HP}}[k] \cdot \text{COP}[k] + Q_{\tau,h}^{\text{oil}}[k] \right), \quad \forall k \in K, \forall \tau \in \mathbf{T}, h \in \mathcal{H}_\tau \quad (7e)$$

$$T_{\tau,h}^m[k+1] = T_{\tau,h}^m[k] + \frac{\Delta t}{C_{\tau,h}^m} \left(H_{\tau,h}^m \cdot (T_{\tau,h}^a[k] - T_{\tau,h}^m[k]) \right), \quad \forall k \in K, \forall \tau \in \mathbf{T}, h \in \mathcal{H}_\tau \quad (7f)$$

$$T_{\min}^a \leq T_{\tau,h}^a[k] \leq T_{\max}^a, \quad \forall k \in K, \forall \tau \in \mathbf{T}, h \in \mathcal{H}_\tau \quad (7g)$$

$$P_{\min}^{\text{HP}} \leq P_{\tau,h}^{\text{HP}}[k] \leq P_{\max}^{\text{HP}}, \quad \forall k \in K, \forall \tau \in \mathbf{T}, h \in \mathcal{H}_\tau \quad (7h)$$

$$0 \leq Q_{\tau,h}^{\text{oil}}[k] \leq Q_{\max}^{\text{oil}}, \quad \forall k \in K, \forall \tau \in \mathbf{T}, h \in \mathcal{H}_\tau \quad (7i)$$

$$T_{\tau,h}^a[1] = T_{\tau,h}^a[K+1] \quad (7j)$$

$$P_{\tau,h}^{\text{HP}}[k] = 0 \quad \text{include if } \min_{t \in \text{day}} \{T_o(t)\} < T_{\min}^o, \quad (7k)$$

$$Q_{\tau,h}^{\text{oil}}[k] = 0 \quad \text{include if } \min_{t \in \text{day}} \{T_o(t)\} \geq T_{\min}^o$$

B. Criteria Assessment

The generation and consumption data obtained from the system model is then used to calculate the impact of different transition pathways using following criteria.

1) *Technological Criteria*: The technological assessment considers the impact of intelligent coordination of resources or the addition renewable resources to the existing system.

a) *Infrastructure Upgrade Factor (IUF)*: This criterion assesses the average infrastructure upgrade factor needed for each transition pathway. The required capacity C_i^{up} is based on the 95th percentile of annual data, rounded to the nearest commercially available size. The IUF is then calculated as (8), where, C_r^{up} and C_r^{orig} are the upgrade and original capacities in kVA or kW of r^{th} resource, \mathcal{R} indicates the total resources.

$$\text{IUF} = \sum_{r \in \mathcal{R}} \text{UF}_r / |\mathcal{R}|, \quad (8)$$

b) *Resource Adequacy*: This criterion extends the traditional $N - 1$ reliability metric—which assumes full failure of a single resource—by accounting for partial operation. Specifically, it measures the percentage of time an additional resource is required, offering a more granular view of system reliability.

2) Economic Criteria:

a) *Additional Infrastructure Cost*: This represents the cost incurred due to capacity upgrades necessitated by the transition pathways. These upgrades may include transformer replacements, battery storage expansion, or additional generation capacity required to support the integration of renewable energy sources and electrification measures.

b) *Electricity Rate (R)*: The electricity rate, denoted by R , is determined by the ratio of the total generation cost to the total electricity sold. Electricity generation cost consists of fuel cost and non-fuel cost.

$$\text{Electricity rate (R)} (\$/\text{kWh}) = \frac{\text{Total generation cost}}{\text{Total kWh sold}}. \quad (9)$$

In some places, Independent Power Producers (IPPs), such as locally owned renewable energy plants and battery storage systems, supply electricity to the local utility. The inclusion

of renewable energy in the system can impact the electricity rate. The revised formula for determining the electricity rate in the presence of IPPs is:

$$R = \frac{\text{Fuel cost} + \text{Non-fuel cost} + \text{IPP purchase cost}}{\text{Total kWh sold}}, \\ = \frac{C_f \frac{D_g}{\eta_g} + C_{\text{nf}} + R_g \times R_{\text{IPP}}}{\text{Total kWh sold}}, \quad (10)$$

Here, C_f is the fuel cost per gallon, η_g is generator efficiency (kWh/gallon), D_g is total fossil-based generation, R_g is renewable energy purchased at rate R_{IPP} , and C_{nf} covers non-fuel operational costs.

c) *Electricity Rate Allowance (ERA)*: In regions with high electricity production costs, subsidies—referred to as electricity rate allowances (ERA)—help reduce the cost burden on consumers by offsetting the difference from baseline grid rates [10]. These subsidies typically apply to eligible residential and commercial users up to a monthly consumption cap. The ERA is calculated based on electricity generation costs, which include fuel prices, non-fuel costs, and the mix of energy sources. A reimbursement rate is applied when the electricity rate exceeds a baseline reference rate, following:

$$\text{ERA} = (\min[R, R_{\max}] - R_{\text{base}}) \times \eta_{\text{ERA}}, \quad (11)$$

where R_{\max} is the reimbursement cap, R_{base} is the reference rate from larger grids, and η_{ERA} is the efficiency factor.

d) *Average annual electricity cost per house*: The average annual electricity cost per household is calculated using monthly consumption and applicable subsidies. Based on total residential usage, the average monthly consumption per household is determined.

In areas with electricity rate allowances (ERA), eligible consumption is computed by subtracting the allowance limit from total monthly use. The annual cost per household is then given by:

$$\text{ERA Eligible kWh} \times (R - \text{ERA}) + \text{Non-eligible kWh} \times R$$

e) *Average annual heating (non-electric) cost per house*: Annual non-electric heating costs are determined based on the amount of fuel required for space heating. The total annual heating cost is calculated as the product of the fuel consumption and the prevailing fuel price per unit.

3) *Environmental Criteria*: The environmental assessment focuses on equivalent carbon dioxide (CO_{2e}) emissions and air quality, specifically PM2.5 levels, using emission factors from the AP42 guidelines. The CO_{2e} emissions from diesel generation are calculated as:

$$\text{CO}_{2e} = (\text{CO}_2^{\text{EI}} \times \text{CO}_2^{\text{GWP}} + \text{CH}_4^{\text{EI}} \times \text{CH}_4^{\text{GWP}} + \text{N}_2\text{O}^{\text{EI}} \times \text{N}_2\text{O}^{\text{GWP}}) D_g, \quad (12a)$$

$$\text{PM}_{2.5} = \text{PM}_{2.5}^{\text{EI}} D_g, \quad (12b)$$

where CO_2^{EI} , CH_4^{EI} , and $\text{N}_2\text{O}^{\text{EI}}$ are the emission indices (lb/mmBtu) for respective greenhouse gases, CO_2^{GWP} , CH_4^{GWP} , and $\text{N}_2\text{O}^{\text{GWP}}$ are their global warming potential values considering 100 years time horizon, and D_g is the energy generated from diesel (mmBtu). When considering heating fuel,

TABLE I
EMISSION INDEX AND GLOBAL WARMING POTENTIAL (GWP) VALUES

Diesel type	Emission Index (EI) (kg/mmBtu)			Global Warming Potential (GPW)		
	CO ₂	CH ₄	N ₂ O	CO ₂	CH ₄	N ₂ O
No.2	73.96	0.003	0.0006	1	28	265
No.1	73.25	0.003	0.0006	1	25	298

D_g refers to the heating energy generated in mmBtu, with emission factors provided by AP42 for the specific fuel type.

4) Social Criteria:

a) *Energy Burden*: This metric is the percentage of gross household income spent on energy costs [34]. When individual income data is unavailable, the median household income is used [35].

b) *Energy Poverty*: Energy poverty refers to lack of access to reliable and affordable energy [34]. It is assessed using surveys on heating-related hardships, e.g., going without heat, unaffordable fuel, or lack of firewood access. These responses are used to compute the Energy Poverty Index (EPI) as:

$$EPI_{\text{base}} = \frac{1}{N} \sum_{i=1}^N X_i, \quad (13)$$

where N is the number of survey indicators and X_i is the fraction reporting a specific hardship.

For transition pathways, EPI is adjusted based on energy cost reductions:

$$EPI_{\text{TP}} = EPI_{\text{base}} \times (1 - \text{cost savings factor}_{\text{TP}}). \quad (14)$$

C. Multi-criteria Decision Analysis (MCDA)

A decision analysis framework is used to evaluate trade-offs between different transition pathways and to assess how benefits are distributed across scenarios. The impact of each transition pathway is influenced by stakeholder preferences, which determine the weights applied in the weighted sum method. Equation (15) presents the calculation of the overall index using this approach.

In this formulation, S^p represents the score for the p^{th} transition pathway, c denotes the criteria index, w_c is the weight assigned to the c^{th} criterion, and \hat{C}_c^p is the normalized score of each criterion for the considered transition pathway.

$$S^p = \frac{1}{N} \sum_{c=1}^N w_c \hat{C}_c^p \quad \forall p \in \text{TP} \quad (15)$$

Since the criteria indices (C_c^p) are measured in different units across various criteria, they are normalized using min-max scaling [36], as shown in Equation (16). This normalization ensures that all criteria indices are dimensionless and comparable on a standardized scale between 0 and 1.

In (16), C_c^p represents the value of the c^{th} criterion under the transition pathway p . The terms $C_{c,b}$ and $C_{c,w}$ denote the best and worst values of the c^{th} criterion across all transition pathways, respectively. For all criteria except the electricity rate allowance level, $C_{c,b}$ corresponds to the minimum value, and $C_{c,w}$ corresponds to the maximum value. For the electricity rate allowance level, $C_{c,b}$ represents the maximum value, while $C_{c,w}$ represents the minimum value. The absolute value

ensures non-negativity, and the result lies within the range $[0, 1]$.

$$\hat{C}_c^p = \left| \frac{C_c^p - C_{c,w}}{C_{c,b} - C_{c,w}} \right| \quad \forall p \in \text{TP} \quad (16)$$

III. CASE STUDY

The proposed framework is applied to the remote Inupiaq communities of Shungnak and Kobuk in Alaska (69°N), located above the Arctic Circle along the Kobuk River. Though 10 miles apart, their grids are connected via an AC tie line, with Shungnak supplying power to Kobuk. Kobuk has a backup diesel generator used only in emergencies. For this study, they are modeled as a single system, comprising 69 and 47 households, respectively, as of 2022 [37], [38].

A. Data collection

The data used for the TEES assessment framework can be grouped into five main categories:

- 1) **Existing energy system infrastructure**: Includes details of the electrical distribution network (Sec III-C) such as transformer capacities, diesel generators, solar PV systems, and battery storage. The Alaska Village Electric Cooperative (AVEC), which serves the communities of Shungnak and Kobuk, provided this data. Relevant data is summarized in Fig. 3 and Table II.
- 2) **Time-series operational data**: Actual hourly generation and consumption profiles for diesel generators, PV panels, batteries, and loads (c.f. Fig. 4) for the year 2023 were obtained from the Agito microgrid controller, provided by the Northwest Arctic Borough (NAB), a local govt. body.
- 3) **Heat pump and household parameters**: HP specifications are sourced from manufacturer datasheets and literature [32]. Details are provided in Table III. Temperature-dependent COP values come from [33], and outdoor temperature data is taken from weather station records.
- 4) **Financial data and assumptions**: Includes historical fuel prices, subsidy values, ERA limits, and economic parameters provided by the NAB. The base system cost is \$1.3 million [39]. Additional costs due to transformer upgrades and solar/battery installations are estimated based on the required upgrade capacity [40], [41]. ERA values use $E_{\text{base}} = 0.1958$ \$/kWh, $E_{\text{max}} = 1$ \$/kWh, and $\eta_{\text{ERA}} = 95\%$, given by Alaska Energy Authority. IPP sales rate is 0.6 \$/kWh and a generator fuel (diesel) cost is 10.17 \$/gallon [39]. Average household energy and heating costs are calculated based on monthly electricity consumption and fuel needs. In the existing system (no HP case), average household uses 500 gallons/year at \$16.14/gallon.
- 5) **Social data**: Energy poverty is assessed using a 2022 heating survey of yes/no questions by the NANA Regional Corporation and McKinley Research Group. It included 54 respondents (15% of total population). Indicators such as heating interruptions (43%), inability to afford fuel/electricity (36%), inability to gather or chop firewood (58%), and lack of firewood access (23%) are used to compute the EPI. A median household income of \$65,000, from Census data, is used to calculate the energy burden.

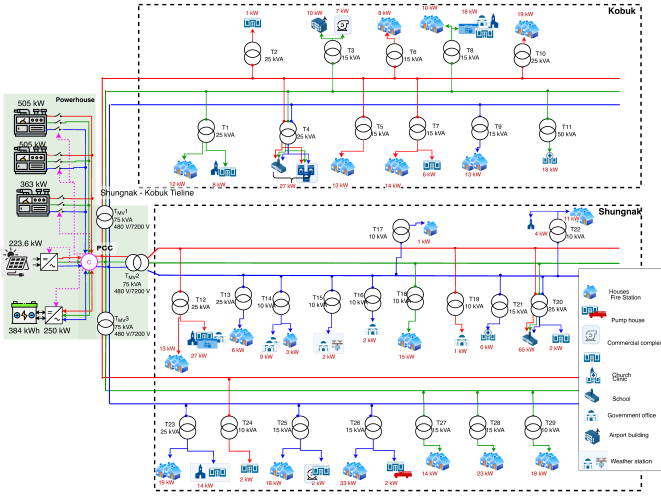


Fig. 3. Electrical system block diagram of Shungnak-Kobuk microgrid

B. Transition Pathways (TP)

These fuel-dependent communities [12] are evaluated across four transition pathways to assess TEES benefits: TP1-no heat pumps (baseline), TP2 - uncoordinated HPs, TP3 - coordinated HPs, and TP4 - HPs with expanded solar PV. Each pathway explores (a) 18 and (b) 12 MBtu/h HPs.

1) *Transition Pathway 1 (TP1): No Heat Pumps (Existing System)*: Represents the current state, where no heat pumps are installed. Households rely on conventional heating methods such as furnaces, wood stoves, and Toyo stoves [12].

2) *Transition Pathway 2 (TP2): Uncoordinated Heat Pumps*: All households are equipped with federally funded heat pumps of either 18 MBtu/h (TP2a) or 12 MBtu/h (TP2b) capacity. These are modeled as in Section III-C1, and the resulting additional demand is used to solve the economic dispatch problem (6). This scenario follows the heat pump model in (7), excluding the optimization terms (7a) and (7b).

3) *Transition Pathway 3 (TP3): Coordinated Heat Pumps*: 18 MBtu/h (TP3a) or 12 MBtu/h (TP3b) HPs are intelligently coordinated to reduce transformer loading using the optimization algorithm described in Section II-A3.

4) *Transition Pathway 4 (TP4): Heat Pumps with Expanded Solar PV*: Builds on the coordinated HP scenario by adding 250 kW of community solar PV. Performance is evaluated for both 18 MBtu/h (TP4a) and 12 MBtu/h (TP4b) HP sizes.

C. System Model

Fig. 3 shows the Shungnak-Kobuk microgrid, powered by three diesel generators (505 kW, 363 kW, 505 kW) totaling 1,373 kW[37], a 223.6 kW solar PV system (SolarEdge SE100K), and a 384 kWh battery with a 250 kW converter (Blue Planet LX, EPC PD250) [42]. A microgrid controller (Ageto ARC), labeled ‘C’ in the figure, manages power distribution. Magenta dotted lines indicate control signals; solid lines represent three-phase power lines (red, green, blue). Transformer capacities and residential loads are detailed in Table II.

Fig. 4 shows 5-minute interval data for 2023. During winter, PV generation is minimal, and diesel supplies the full demand. The generator operated at 34% capacity, while solar PV was

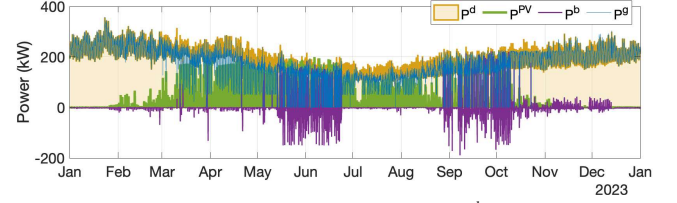


Fig. 4. Shungnak-Kobuk PCC power data for 2023: P^d is total demand (kW), P^g diesel generation, P^{PV} solar output, and P^b battery power (negative: charging; positive: discharging)

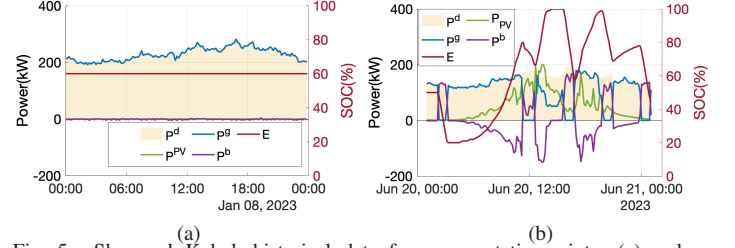


Fig. 5. Shungnak-Kobuk historical data for representative winter (a) and summer (b) days. E represents battery’s State of Charge (SOC).

utilized at only 10%, highlighting seasonal variation. Fig. 5 shows combined demand and generation profiles for Shungnak and Kobuk on representative winter and summer days, selected at the 90th and 10th percentiles of annual temperature. On the winter day (Fig. 5a), PV output is near zero, the battery stays idle, and diesel meets the full load, including the annual peak. On the summer day (Fig. 5b), demand is lower, PV supports load and charges the battery, and diesel remains off for four intervals—solar and battery meet the full demand for 100 minutes.

1) Component Models:

a) *Diesel generator model*: The generator is modeled as indicated in Section II-A. The fuel used is No. 2 diesel fuel [43] with a cost of \$10.17 per gallon [39]. This resulting fuel cost curve revealed a linear cost curve for the generator, represented by, $700 \times P^g$.

For this case study, the solar PV power output is provided as data and used directly, eliminating the need for a solar PV model.

b) *Battery model*: A battery is modeled as indicated in Section II-A. \underline{E} and \overline{E} are set to 20% and 90%, respectively, η^b is 95%, and $\Delta t = 5$ min—chosen to balance SoC accuracy with computational efficiency.

c) *Heat pump*: A HP is modeled as indicated in Section II-A. The house parameters (C^a , U^a , H^m , and C^m) are adapted from [32] where the authors generated the parameters using GridLAB-D with $\pm 10\%$ random variation for a house size of 2500 sq.ft. The parameters are scaled proportionately to reflect the typical 1000 sq. ft. houses for Shungnak and Kobuk.

The Shungnak-Kobuk electrical system is simulated considering optimal energy dispatch, $\alpha = 700$ and $\gamma = 0.1$, (Section II-A2) and using the diesel generator and battery models. The results obtained are validated with the historical diesel generation and battery power variation data (Fig. 4) for the base case (case with no heat pumps).

TABLE II
RATED CAPACITY AND MAXIMUM LOAD AT THE LV TRANSFORMERS WITH RESIDENTIAL LOADS

Transformer	T1	T2	T3	T4	T5	T6	T7	T8	T9	T10	T11	T12	T13	T14	T15	T16	T17	T18	T19	T20	T21	T22	T23	T24	T25	T26	T27	T28	T29
Capacity (kVA)	25	25	15	25	15	15	15	15	15	25	50	25	25	10	10	10	10	10	10	15	25	10	25	10	15	15	15	15	10
# Houses	10	-	-	-	8	6	6	5	5	7	4	-	2	1	-	-	1	6	-	-	-	4	7	-	7	14	8	9	6
Estimated Demand (kW)	12	-	-	-	13	8	14	10	13	19	-	13	6	3	-	-	1	15	-	-	-	11	19	-	18	33	14	23	18

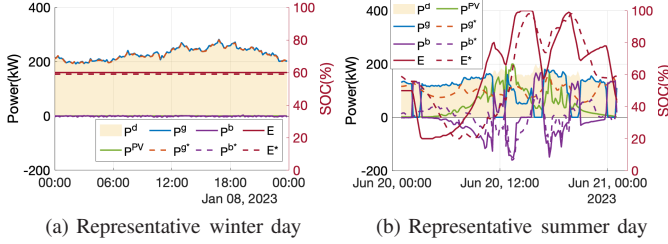


Fig. 6. Validation of the economic dispatch algorithm with the base case. Solid lines indicate historical data whereas dashed lines indicate optimized values.

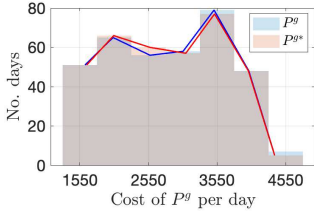


Fig. 7. Variation in daily cost of historical value P^g and optimized value P^{g*} .

IV. RESULTS

A. Transition Pathway 1 (No heat pump):

This baseline pathway uses 2023 data for demand, diesel, solar PV, and battery power (Fig. 4). Historical values of P^{PV} and P^d are used in the optimal dispatch formulation (6), and results (P^{g*} , P_c^{b*} , P_d^{b*}) are compared with actual data. The problem is modeled as a mixed-integer linear program (MILP) and solved daily for a full year using Julia JuMP with Gurobi, totaling 288 binary variables per day. The full-year solution time is under a minute.

Fig. 6 compares optimized and historical values for representative winter and summer days. Here, P^g , P^b , and SOC (E) are historical, while starred variables are optimized results. Generator cost differences are minimal—0.4% (winter), 0.07% (summer), with max and average daily differences of 8% and 1.2%. Annual cost from P^{g*} is \$4k (4%) lower than historical P^g , as shown in the histograms in Fig. 7, validating the ED model and confirming near-optimal historical operations.

The average generator efficiency from the cost curve and ED results is 11.73 kWh/gallon. For emissions, the generator contributes 5118 MMBtu and heating uses 58,000 gallons of fuel. These values are used to compute the TEES indices.

B. Transition Pathway 2 (Uncoordinated heat pumps):

For the uncoordinated HP scenario, the Shungnak-Kobuk system is simulated with HPs in each house (Section III-B). HP specifications are in Table III, with the cutoff temperature T_{min}^o set to the minimum rated outdoor temperature. A variable COP, dependent on outdoor temperature, is used from [33], better reflecting local conditions than manufacturer-rated values.

Fig. 8a shows power and temperature profiles on a representative winter day for 18 MBtu/h (TP2a) uncoordinated

TABLE III
HEAT PUMP PARAMETERS CONSIDERED FOR STUDY

Parameter	Value	Value
Size (MBtu/h)	18	12
Rated power (kW)	4.14	2.81
Indoor operating temp ($^{\circ}$ C)	14 - 22	14 - 22
Min rated outdoor operating temp ($^{\circ}$ C)	-30	-20

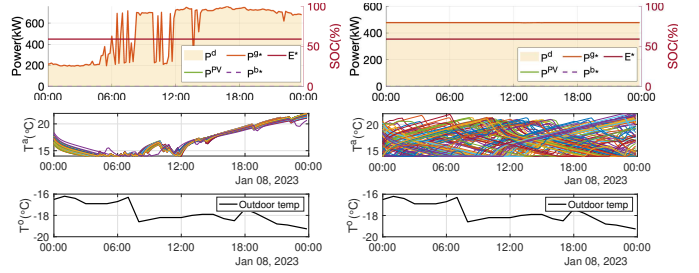


Fig. 8. Power, indoor (T^i) and outdoor (T^o) temperature for representative winter day for 18 MBtu/h uncoordinated (TP2a) and coordinated (TP3a) HPs.

HPs. The uncoordinated HPs trigger sharp demand peaks (up to 500 kW) due to simultaneous activation, stressing the generator. Indoor temperatures vary across homes, where each color represents the temperature of an individual house. When outdoor temperature drops below T_{min}^o , HPs shut off and oil heating is used.

The study is conducted for the full year of 2023, and the outputs are used to compute performance indices. A similar analysis is performed for the 12 MBtu/h (TP2b) HP case, though plots are omitted for brevity. Average generator efficiency for TP2 is 11.93 kWh/gallon for 18 MBtu/h HPs and 12 kWh/gallon for 12 MBtu/h HPs, based on the generator cost curve and ED results. A detailed evaluation of criteria performance follows in the next section.

C. Transition Pathway 3 (Coordinated heat pumps):

Fig. 8b shows power and temperature profiles on a representative winter day for 18 MBtu/h coordinated HPs (TP3a), with the cutoff temperature matching the rated minimum. Unlike uncoordinated operation, coordination results in a flatter power profile, minimizing peaks in P^g and easing generator strain.

The coordinated setup maintains consistent power demand and indoor temperatures across households (each color in Fig. 8b represents one home), improving thermal comfort and generator efficiency. The initial indoor temperature differs from the uncoordinated case as it reflects the more uniform end-of-day temperature distribution from the previous day.

Fig. 9 shows the annual diesel generator output distribution for 18 and 12 MBtu/h HPs under uncoordinated and coordinated control, with cutoff temperatures set to the rated minimum (Table III). The red dashed line marks the generator's max capacity. Coordination reduces peak generation, allowing one generator to serve the load while reserving others

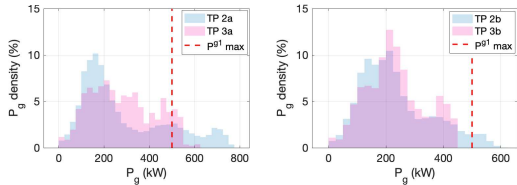


Fig. 9. Distribution of yearly generation by the diesel generator with (a) 18 MBtu/h and (b) 12 MBtu/h integration.

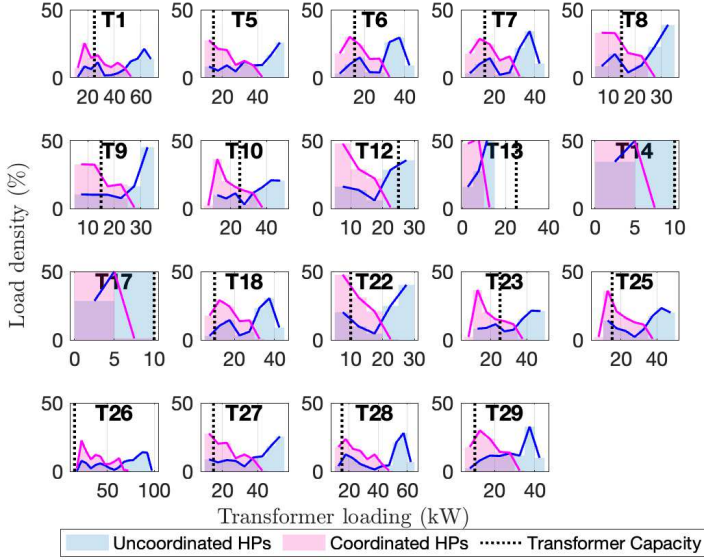


Fig. 10. Load distribution on LV transformers for 18 MBtu/h HPs.

for backup, thereby enhancing reliability. It also smooths generation profiles, reducing peaks and distributing load more evenly—improving efficiency and reducing generator wear. In addition to total capacity, transformer-level loading is analyzed for coordinated and uncoordinated HPs. Fig. 10 shows annual load distributions for 18 MBtu/h HPs across the transformers. Load density (%) is plotted against power (kW), with transformer capacity shown by dotted lines. Uncoordinated HPs lead to wider, higher load spreads, exceeding capacity on 15 of 19 transformers. Coordination narrows the distribution, reducing peak loads and transformer stress, though some upgrades are still required. The 12 MBtu/h HPs exhibit similar trends, although the overall load density is lower compared to the 18 MBtu/h HPs.

Fig. 11 shows transformer capacity upgrades for each transition pathway. TP1 (base case) reflects original ratings. TP2a (uncoordinated 18 MBtu/h HPs) demands the highest upgrades, while TP3b (coordinated 12 MBtu/h HPs) requires the least. TP2b (uncoordinated 12 MBtu/h HPs) and TP3a (coordinated 18 MBtu/h HPs) have similar upgrade needs. TP4a and TP4b (solar PV expansions) are excluded since solar capacity doesn't impact transformer sizing; their requirements match TP3a and TP3b, respectively. All three MV transformers need upgrades, with TP2a requiring the most and TP3b the least. The average upgrade factor (8) ranges from 3 to 1.7, allowing calculation of additional infrastructure costs per pathway.

The year-long analysis reveals that coordinated HPs produce a smoother P_g^e profile and slightly better generator efficiency. Using the generator cost curve and ED results, TP3 yields average efficiencies of 12.23 and 12.13 kWh/gallon for 18 and 12 MBtu/h HPs, respectively. These P_g^e values are used

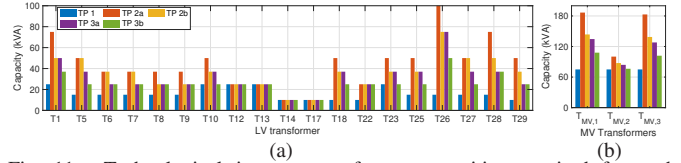


Fig. 11. Technological impact: transformer capacities required for each transition pathway. (a) LV transformers (b) MV transformers.

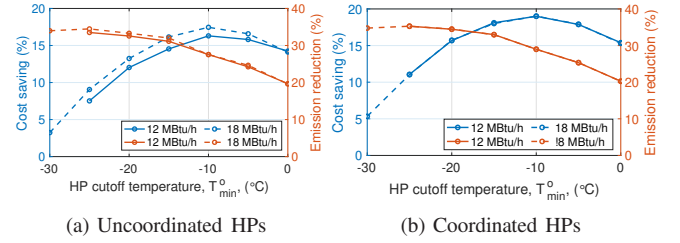


Fig. 12. Variation in cost saving and CO_2e emission reduction w.r.t. HP cutoff temperature

to compute performance indices, highlighting improved efficiency and reduced operating costs (Table IV).

D. Transition Pathway 4 (Solar PV capacity expansion):

This section analyzes the impact of doubling existing solar capacity on system performance, in combination with heat pump (HP) adoption. Both coordinated and uncoordinated HP operations are evaluated for 18 MBtu/h and 12 MBtu/h units; however, only coordinated results are shown in the table IV, as uncoordinated HPs yield slightly higher values across most criteria.

During summer, HP usage is low, resulting in similar demand levels with or without HPs. However, the increased solar generation requires significantly more storage—approximately three times the current battery capacity—to capture surplus energy and minimize curtailment. While this would substantially raise system costs, the analysis assumes the expanded PV is fully government-funded and incurs no additional expense. In contrast, winter performance remains largely unaffected by added PV capacity due to minimal solar availability during the coldest months when HPs are most active. Thus, solar expansion has limited influence on winter performance.

V. DISCUSSION

This section provides a comparative discussion on the TEES assessment indices for the considered transition pathways. Operating HPs with cutoff temperature equal to their minimum outdoor operating temperature requires significant infrastructure upgrades, leading to increased costs. To identify the optimal cutoff temperature (T_{\min}^o) for HP operation, the TEES assessment framework is rerun across different cutoff temperatures. As shown in Fig. 12, cost savings peak at -10°C , while emissions reduction is highest at -25°C . The sharp decline in savings at -25°C indicates that -10°C offers the best trade-off between economic and environmental performance. The results also highlight the value of dual heating systems that switch between HPs and conventional sources based on outdoor temperature. Coordinated HPs provide slightly higher savings than uncoordinated ones, though both follow similar trends. Given that cost savings peak at $T_{\min}^o = -10^\circ\text{C}$, Table IV presents TEES outcomes for all transition pathways

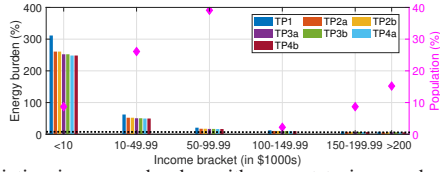


Fig. 13. Variation in energy burden with respect to income bracket

at this optimal cutoff, including 18 and 12 MBtu/h HPs under both strategies and with expanded solar PV. For uncoordinated HPs, annual household energy cost savings reach 17% (TP2a) and 16% (TP2b) compared to the base case (TP1). Coordination improves savings to 19% for both HP sizes. With expanded solar (TP4b), savings rise to 20%. These reductions stem from shifting from costly fuel to cheaper electricity. Non-electric heating costs remain constant across all HP scenarios, as the cutoff temperature is fixed at -10°C . From an environmental perspective, HP integration reduces CO_{2e} emissions by up to 28% (uncoordinated) and 29% (coordinated). PV capacity expansion further improves the reduction to 35%. In terms of social benefits, both energy burden and poverty decline with HP adoption. Energy burden drops from 24% in the base case to 20% with uncoordinated HPs, with similar reductions under coordination. Energy poverty also decreases across all pathways, lowest for the 12 MBtu/h coordinated HP. Fig. 13 shows energy cost as a percentage of income across brackets, with population distribution marked by pink diamonds and the burden limit by a black dotted line. While 74% of the population remains above the burden threshold, HP integration (TPs 2–4) notably reduces burden for low-income groups.

The table also includes transition scores, computed using equal weights for all criteria as per Section II-C. TP1 ranks lowest, while TP4b ranks highest due to excluded solar PV installation costs. If these costs are included, TP3b becomes the top-ranked option. Overall, scenarios with 12 MBtu/h HPs achieve higher scores than 18 MBtu/h HPs. Even uncoordinated 12 MBtu/h HPs (TP2b) improve the score by 8%, with a 21% boost under coordination (TP3b). Adding solar (TP4b) raises the score another 5%. The wider gap between coordinated and uncoordinated HPs reflects higher infrastructure and transformer upgrade costs in the latter.

Overall, coordinated HP pathways offer more balanced improvements across economic, environmental, and social metrics, while uncoordinated pathways primarily yield targeted gains like CO_{2e} reduction. The optimal transition pathway depends on community priorities. For minimal coordination, TP1 \rightarrow TP2a/TP3a \rightarrow TP4a offers a simpler route with substantial benefits. In contrast, TP1 \rightarrow TP2b/TP3b \rightarrow TP4b provides a more integrated, balanced transition but requires greater system management. This choice also hinges on infrastructure availability—coordinated strategy demands reliable communication networks, which may be challenging in remote areas.

VI. CONCLUSION

This study developed a comprehensive techno-economic, environmental, and social (TEES) assessment framework to

evaluate energy transition pathways. The framework provided a structured approach to assess infrastructure requirements, energy costs, emissions reductions, and social equity impacts, enabling informed decision-making for sustainable electrification.

The framework was applied to the remote Alaskan communities of Shungnak and Kobuk to evaluate three transition pathways incorporating heat pump and battery integration, intelligent coordination of resources, and expanded community solar PV capacity. Results showed that heat pumps significantly reduced CO_2 emissions and total energy costs, despite increasing electricity demand. Coordinated HP operation further enhanced these benefits by minimizing peak loads, improving grid reliability, and reducing annual energy costs by up to 20%. Integrating additional solar PV amplified these gains, achieving a 35% reduction in emissions and greater energy affordability. The results also highlight the benefits of dual heating systems, where households retain both conventional heating sources and HPs, strategically staging them based on outdoor temperature for improved economic efficiency.

The proposed TEES assessment framework is designed to be flexible and scalable, enabling its application to a wide range of regions with varying energy challenges. Future work will expand this analysis to compare transition pathways across diverse communities, incorporating differences in resource availability, infrastructure, and socio-economic conditions.

ACKNOWLEDGMENT

This work was supported by the generous funds from Sloan Foundation and the Catalyst Award from the Gund Institute of the Environment at the University of Vermont. We are profoundly grateful to the Tribe of Shungnak and the Tribe of Kobuk where this research is based. This work would not have been possible without the support of Billy Lee from Shungnak, Darren Westby and Bill Stamm at AVEC, the NANA Regional Corporation, and the Northwest Arctic Borough who provided the data to do this analysis and for their generous guidance and ongoing feedback on this work. Additionally we are grateful for the monthly debriefings we have had with our collaborators Michelle Wilbur, Shivani Bhagat, and Christie Hauptert at the Alaska Center for Energy and Power, at the University of Alaska Fairbanks.

REFERENCES

- [1] D. Gielen, F. Boshell, D. Saygin, M. D. Bazilian, N. Wagner, and R. Gorini, “The role of renewable energy in the global energy transformation,” *Energy strategy reviews*, vol. 24, pp. 38–50, 2019.
- [2] F. W. Geels, B. K. Sovacool, T. Schwanen, and S. Sorrell, “Sociotechnical transitions for deep decarbonization,” *Science*, vol. 357, no. 6357, pp. 1242–1244, 2017.
- [3] B. K. Sovacool, “How long will it take? conceptualizing the temporal dynamics of energy transitions,” *Energy research & social science*, vol. 13, pp. 202–215, 2016.
- [4] R. Fouquet, “Historical energy transitions: Speed, prices and system transformation,” *Energy research & social science*, vol. 22, pp. 7–12, 2016.
- [5] J. Markard, “The next phase of the energy transition and its implications for research and policy,” *Nature Energy*, vol. 3, pp. 628–633, Aug. 2018. Publisher: Nature Publishing Group.

TABLE IV
TECHNOLOGICAL, ECONOMIC, ENVIRONMENTAL, AND SOCIAL CRITERIA ASSESSMENT FOR DIFFERENT TRANSITION PATHWAYS. $T_{\text{MIN}}^{\circ} = -10^{\circ}\text{C}$

Criterion	No Hp	Uncoordinated HPs		Coordinated HPs		PV capacity expansion		
	TP1	18 MBtu/h TP2a	12 MBtu/h TP2b	18 MBtu/h TP3a	12 MBtu/h TP3b	18 MBtu/h TP4a	12 MBtu/h TP4b	
Technological	Avg. transformer upgrade factor	1	2.6	2.1	1.7	1.6	1.7	1.6
	Resource Adequacy(%)	0	0.1	0.5	0	0	0	0
Economic	Add'l infrastructure cost	0	\$196k	\$175k	\$121k	\$110k	\$121k	\$110k
	Retail electricity rate (\$/kWh)	0.99	0.97	0.96	0.97	0.97	0.94	0.94
	PCE level (\$/kWh)	0.76	0.73	0.73	0.74	0.74	0.71	0.71
	Avg annual electricity cost per household	\$7.5k	\$9.23k	\$9.4k	\$8.99k	\$8.99k	\$8.79k	\$8.79k
	Avg annual (non-ele) heating cost per house	\$8.07k	\$3.63	\$3.63k	\$3.63k	\$3.63k	\$3.63k	\$3.63k
	Total annual energy cost per household	\$15.6k	\$12.8k	\$13.0k	\$12.6k	\$12.6k	\$12.4k	\$12.4k
	% saving	–	17.5%	16.3%	19.0%	19.0%	20.3%	20.3%
Environmental	Annual CO _{2e} emission (metric ton)							
	From power gen	372	427	433	419	419	366	366
	From heating	594	267	267	267	267	267	267
	Total reduction	–	27.5%	27.5%	28.9%	28.9%	34.5%	34.5%
	PM2.5 (µg/m3)	17.9	12.9	13.0	12.7	12.7	11.8	11.8
Social	Energy Burden	23.9%	20.0%	20.0%	19.4%	19.4%	19.1%	19.1%
	Energy Poverty	40%	33.1%	33.5%	32.4%	32.4%	30.9%	30.9%
Transition score		0.44	0.46	0.52	0.71	0.73	0.76	0.78

- [6] D. P. Van Vuuren, E. Stehfest, D. E. Gernaat, M. Van Den Berg, D. L. Bijl, H. S. De Boer, V. Daioglou, J. C. Doelman, O. Y. Edelenbosch, M. Harmsen, *et al.*, “Alternative pathways to the 1.5 c target reduce the need for negative emission technologies,” *Nature climate change*, vol. 8, no. 5, pp. 391–397, 2018.
- [7] B. Chen, R. Xiong, H. Li, Q. Sun, and J. Yang, “Pathways for sustainable energy transition,” *Journal of Cleaner Production*, vol. 228, pp. 1564–1571, 2019.
- [8] J. Köhler, F. W. Geels, F. Kern, J. Markard, E. Onsongo, A. Wiecek, F. Alkemade, F. Avelino, A. Bergek, F. Boons, *et al.*, “An agenda for sustainability transitions research: State of the art and future directions,” *Environmental innovation and societal transitions*, vol. 31, pp. 1–32, 2019.
- [9] G. Bridge, S. Bouzarovski, M. Bradshaw, and N. Eyre, “Geographies of energy transition: Space, place and the low-carbon economy,” *Energy policy*, vol. 53, pp. 331–340, 2013.
- [10] M. Arriaga, C. A. Cañizares, and M. Kazerani, “Renewable energy alternatives for remote communities in northern ontario, canada,” *IEEE Transactions on sustainable energy*, vol. 4, no. 3, pp. 661–670, 2013.
- [11] G. Holdmann, D. Pride, G. Poelzer, B. Noble, and C. Walker, “Critical pathways to renewable energy transitions in remote alaska communities: A comparative analysis,” *Energy Research & Social Science*, vol. 91, p. 102712, 2022.
- [12] Northwest Arctic Borough Alaska, “Northwest arctic regional energy plan 2022,” tech. rep., 2022.
- [13] L. Kainiemi, M. Laukkanen, and J. Levänen, “Multi-sectoral interactions in energy transition: Unveiling tensions between sustainability and justice,” *Applied Energy*, vol. 384, p. 125437, 2025.
- [14] Y. Wang, Z. Quan, Y. Zhao, G. Rosengarten, and A. Mojiri, “Techno economic analysis of integrating photovoltaic-thermal systems in ground-source heat pumps for heating-dominated regions,” *Applied Energy*, vol. 377, p. 124677, 2025.
- [15] M. Bilal, F. Ahmad, A. Mohammad, and M. Rizwan, “Techno-economic evaluation and sensitivity analysis of renewable energy based designing of plug-in electric vehicle load considering load following strategy,” *Applied Energy*, vol. 377, p. 124557, 2025.
- [16] S. Jouttijärvi, L. Karttunen, S. Ranta, and K. Miettunen, “Techno-economic analysis on optimizing the value of photovoltaic electricity in a high-latitude location,” *Applied Energy*, vol. 361, p. 122924, 2024.
- [17] L. Herenčić, M. Melnjak, T. Capuder, I. Andročec, and I. Rajšl, “Techno-economic and environmental assessment of energy vectors in decarbonization of energy islands,” *Energy conversion and management*, vol. 236, p. 114064, 2021.
- [18] D. Roy, S. Zhu, R. Wang, P. Mondal, J. Ling-Chin, and A. P. Roskilly, “Techno-economic and environmental analyses of hybrid renewable energy systems for a remote location employing machine learning models,” *Applied Energy*, vol. 361, p. 122884, 2024.
- [19] X. Garcia-Casals, R. Ferroukhi, and B. Parajuli, “Measuring the socio-economic footprint of the energy transition,” *Energy Transitions*, vol. 3, no. 1, pp. 105–118, 2019.
- [20] M. A. Abdoulaye, S. Waita, C. W. Wekesa, and J. M. Mwabora, “Optimal sizing of an off-grid and grid-connected hybrid photovoltaic-wind system with battery and fuel cell storage system: a techno-economic, environmental, and social assessment,” *Applied Energy*, vol. 365, p. 123201, 2024.
- [21] A. S. Gaur, D. Z. Fitiwi, and J. Curtis, “Heat pumps and our low-carbon future: A comprehensive review,” *Energy Research & Social Science*, vol. 71, p. 101764, 2021.
- [22] P. R. White, J. D. Rhodes, E. J. Wilson, and M. E. Webber, “Quantifying the impact of residential space heating electrification on the texas electric grid,” *Applied Energy*, vol. 298, p. 117113, 2021.
- [23] A. M. Brockway and P. Delforge, “Emissions reduction potential from electric heat pumps in california homes,” *The Electricity Journal*, vol. 31, no. 9, pp. 44–53, 2018.
- [24] M. Farghali, A. I. Osman, I. M. Mohamed, Z. Chen, L. Chen, I. Ihara, P.-S. Yap, and D. W. Rooney, “Strategies to save energy in the context of the energy crisis: a review,” *Environmental Chemistry Letters*, vol. 21, no. 4, pp. 2003–2039, 2023.
- [25] A. Bloess, W.-P. Schill, and A. Zerrahn, “Power-to-heat for renewable energy integration: A review of technologies, modeling approaches, and flexibility potentials,” *Applied Energy*, vol. 212, pp. 1611–1626, 2018.
- [26] T. A. Deetjen, L. Walsh, and P. Vaishnav, “US residential heat pumps: the private economic potential and its emissions, health, and grid impacts,” *Environmental Research Letters*, vol. 16, no. 8, p. 084024, 2021.
- [27] A. M. Brockway, J. Conde, and D. Callaway, “Inequitable access to distributed energy resources due to grid infrastructure limits in california,” *Nature Energy*, vol. 6, no. 9, pp. 892–903, 2021.
- [28] C. McKenna, P. Vaishnav, and C. Gronlund, “Heating with Justice: Barriers and Solutions to a Just Energy Transition in Cold Climates,” Feb. 2024.
- [29] D. Bogdanov, R. Satymov, and C. Breyer, “Impact of temperature dependent coefficient of performance of heat pumps on heating systems in national and regional energy systems modelling,” *Applied Energy*, vol. 371, p. 123647, 2024.
- [30] Rossol, G. Michael, G. Brinkman, P. Buster, J. Denholm, G. Novacheck, and Stephen, *A National Thermal Generator Performance Database*. NREL Data Catalog. Golden, CO: National Renewable Energy Laboratory, 2018.
- [31] A. Bergen and V. Vittal, *Power Systems Analysis*. Prentice Hall, 2000.
- [32] O. Oyefeso, G. S. Ledva, M. Almassalkhi, I. A. Hiskens, and J. L. Mathieu, “Control of Aggregate Air-Conditioning Load using Packetized Energy Concepts,” in *2022 IEEE Conference on Control Technology and Applications (CCTA)*, pp. 447–454, Aug. 2022. ISSN: 2768-0770.
- [33] “Mini-split heat pumps in alaska: Heat pump calculator algorithms and data,” 2018.
- [34] S. H. Baker, “Anti-resilience: a roadmap for transformational justice within the energy system,” *Harv. CR-CLL Rev.*, vol. 54, p. 1, 2019.
- [35] O. Ma, K. Laymon, M. Day, R. Oliveira, J. Weers, and A. Vimont, “Low-Income Energy Affordability Data (LEAD) Tool Methodology,” Tech. Rep. NREL/TP-6A20-74249, 1545589, July 2019.
- [36] N. Vafaie, R. A. Ribeiro, and L. M. Camarinha-Matos, “Normalization techniques for multi-criteria decision making: analytical hierarchy process case study,” in *Technological innovation for cyber-physical systems: 7th IFIP WG 5.5/SOCOLNET advanced doctoral conference*

on computing, electrical and industrial systems, DoCEIS 2016, Costa de Caparica, Portugal, April 11–13, 2016, Proceedings 7, pp. 261–269, Springer, 2016.

- [37] Northwest Arctic Borough Alaska, “Community profile shungnak,” 2022.
- [38] Northwest Arctic Borough Alaska, “Community profile kobuk,” 2022.
- [39] Alaska Energy Authority, “FY23 PCE statistical report,” 2024.
- [40] Jeremy, “How Much Does a Power Pole Transformer Cost,” Sept. 2024.
- [41] “Larson Electronics - 250 KVA Pad Mount Transformer - 12470Y/7200 Wye-N Primary, 120/240V Delta Secondary - Copper, ONAN/Bell Green,” 2025.
- [42] Ageto Energy, 2021.
- [43] United States Department of Transportation, Bureau of Transportation Statistics, “National Transportation Statistics (NTS),” 2019.